

Experimental evidence of a Mott transition in highly doped two-dimensional confined structures

Mathieu Carras,^{1,2} Vincent Berger,² Xavier Marcadet,¹ and Borge Vinter¹

¹Thales Research and Technology, domaine de corbeville, Orsay F-91404, France

²Laboratoire "Matériaux et Phénomènes Quantiques," Université Denis Diderot Paris 7 case 7021, 2 place Jussieu, Paris 75251, France

(Received 3 September 2004; published 20 December 2004)

Mott transition in a two-dimensional electron gas in a doped GaAs/AlGaAs quantum well is experimentally studied. The impurity band is observed at a doping level up to 10^{18} cm^{-3} . This value is two orders of magnitude higher than the Mott transition in bulk GaAs (about 10^{16} cm^{-3}). This high density Mott transition is explained by a quantitative model involving the donor distribution in the wells.

DOI: 10.1103/PhysRevB.70.233310

PACS number(s): 73.20.Hb, 71.30.+h

The Mott transition is defined as the doping limit over which the population of free carriers in a doped material no longer depends on the temperature.¹ Below this limit, impurity and conduction bands are separated in energy, and above this limit, the material is a semi-metal: impurity and conduction bands are degenerate. In bulk *n*-type GaAs, this transition occurs around a doping level of 10^{16} cm^{-3} .²⁻⁴ Heavily doped AlGaAs/GaAs heterostructures (a few 10^{17} cm^{-3}) are commonly considered as being doped over the Mott transition.

In this report, the transition is experimentally studied in doped AlGaAs/GaAs quantum well (QW) heterostructures. The impurity band is measured to be not degenerate, with the confined ground state for a doping level two orders of magnitude higher than the bulk GaAs Mott transition density. The dependence of the binding energy of an impurity level in a QW was studied by Bastard.⁵ The calculations for a single hydrogenic impurity (located at the QW center) give a binding energy of 13 meV for a 6-nm-wide well that is more than two times higher than in bulk GaAs (about one Rydberg: 5.8 meV). At the Mott transition, the broadening of the impurity band, increasing with the donor density, compensates the binding energy. Because the latter is higher in the QW case with regard to bulk, the Mott transition occurs at a higher doping level.

Recent work has been devoted to the quantification of this limit, but no experimental result has validated these models this far.^{6,7} This study requires doped QWs (and not modulation-doped ones as in most devices). For this purpose, we have used quantum well infrared photodetector (QWIP) structures with the appropriate doping density. Indeed, the result of the study is fundamental for the development of the device, in particular for controlling the cutoff wavelength and quantum efficiency as a function of temperature. We also developed a model that fits very accurately the absorption spectra. This model, together with the low-temperature spectra, informs us about the spatial distribution of the donors in the well, giving interesting nondestructive feedback after the QW growth.

Multi-QW structures of 1 to 100 wells were grown by molecular-beam epitaxy. 5 nm of GaAs wells are separated by 34 nm $\text{Al}_{0.3}\text{Ga}_{0.7}\text{As}$ barriers. Samples 1 and 5 contain 40 QWs doped in their central third to a donor concentration of $2 \times 10^{11} \text{ cm}^{-2}$. The only difference between the two is that

sample 1 has two Si-doped GaAs contact layers on each side of the QW stack. Sample 2 has the same structure, but with one hundred $4 \times 10^{11} \text{ cm}^{-2}$ δ -doped QWs. Sample 3 contains one well only, which is modulation doped with a Schottky barrier that allows the electrical control of the carrier density in the well. Sample 4 is designed to be optically pumped⁸ and provides a large electron density for a low pump power. It contains double QWs, separated with an AlAs barrier. Electron-hole pairs created in the thinner QW are separated: the electron transit to the wider QW through the *X* valley in the AlAs. The resulting spatial separation of holes and electrons provides long lifetime and thus high electron concentration in the wide wells.⁹ For all these samples, absorption spectra were obtained in a Fourier transform infrared spectrometer in a liquid-helium flow cryostat. A multipath geometry with a 45° incidence was used to enhance the intersubband absorption. The nonabsorbed polarization was used as a baseline to normalize the spectra.

In a structure where the donors are located in the well, the lowest energy levels are provided by impurity states (inset of Fig. 1). The following behavior is then expected at low tem-

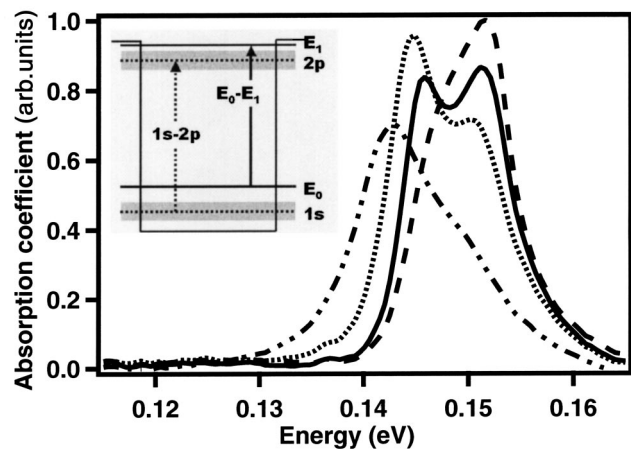


FIG. 1. Absorption spectra of sample 1 multi-QW structure for different temperatures (Dashed: 10 K; Full: 60 K; Dotted: 120 K; Dash-dotted: 240 K). Inset: Doped QW with the different energy levels; the gray area represents the impurity bands caused by the broadening of the impurity levels $1s$ and $2p_z$.

perature: all levels under the Fermi energy are full; the first conduction subband is thus empty, whereas impurity level ($1s$ on Fig. 1) is occupied. As the temperature increases the Fermi distribution smoothes and some electrons leave the $1s$ state for the E_0 one. At ambient temperature, the binding energy (a few meV) becomes small compared to the thermal energy (~ 25 meV), and the electron distribution on the two levels is only proportional to the density of states. In the impurity band, this density is equal to the doping Nd (about 2×10^{11} cm $^{-2}$) and in the first conduction subband the density reaches 10^{13} eV $^{-1}$ cm $^{-2}$ (about 7×10^{11} cm $^{-2}$ for the states between E_0 and $E_0 + 25$ meV, for instance). Therefore, many electrons occupy the conduction ground state at room temperature. The absorption spectrum is the superposition of the spectra of the two transitions $1s \rightarrow 2p_z$ and $E_0 \rightarrow E_1$, whose areas are proportional to the number of electrons on $1s$ and E_0 , respectively (the excited states being considered as nearly empty). Increasing the temperature, the area of the absorption peak associated with the $1s \rightarrow 2p_z$ transition is expected to decrease, whereas the area of the $E_0 \rightarrow E_1$ transition absorption peak increases.

Two maximums separated by 6 meV appear indeed on the spectra measured with sample 1 (doped 2×10^{11} cm $^{-2}$). As expected, the higher energy peak associated with the intra-impurity level transition is dominant at low temperature, and the $E_0 \rightarrow E_1$ peak at low energy dominates at high temperature. The striking difference between our observation and the one made by Helm *et al.*^{10,11} is our very large doping level (10^{18} cm $^{-3}$ with respect to 6×10^{16} cm $^{-3}$ in their case). The difference in energy between the two peaks is equal to 6 meV, and cannot be explained by a Stark effect¹² combined with built-in inhomogeneous electric field. Indeed, the Stark effect in a square QW is a second-order effect.¹³ In addition, many-body effects associated with inhomogeneous carrier density are also expected to have a little impact on the absorption shape, and cannot in any case be responsible for a 6 meV splitting of the absorption peak. To further confirm that this effect is related to the presence of impurities in the well, this result has been compared to other carrier filling mechanisms: modulation doping and optical pumping.

Absorption spectra for the modulation-doped sample 3 are shown in Fig. 2 (left): A single peak is observed at all temperatures, as expected. The variations of the area are due to DX defects caused by the modulation doping, reducing the number of available carriers in some temperature range.¹⁴

The last filling mechanism investigated is optical pumping. We do not see any second peak appearance on the low-temperature spectra (Fig 2; right) for carrier densities from 7×10^9 cm $^{-2}$ up to 1.7×10^{11} cm $^{-2}$. Although much more affected by the noise due to the small size of the optically pumped sample, the higher temperature spectra do not show any two-peak structure.

These results confirm that two distinct peaks are observed only for sample 1, i.e., only in case of doped QWs. QWs are doped at a doping level of 2×10^{11} cm $^{-2}$ in their center, on a width of about 2 nm corresponding to a 10^{18} cm $^{-3}$ density. We also observed a drop of the conduction of the wells at low temperature by two orders of magnitude, interpreted as a transition from conduction band to impurity band conduction. This doping level of 10^{18} cm $^{-3}$ is two orders of magni-

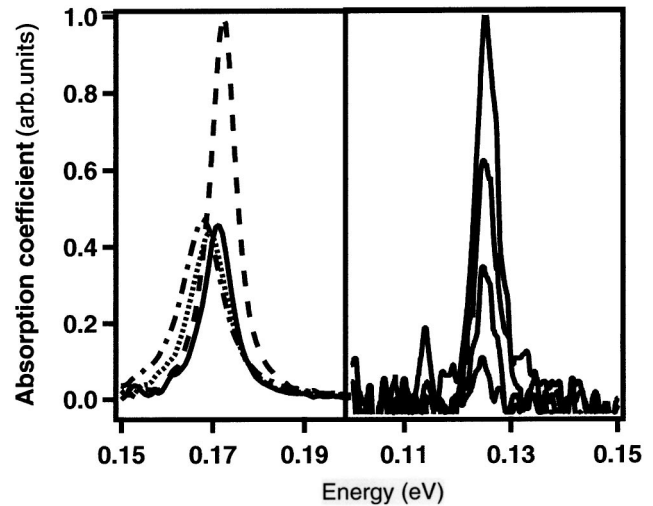


FIG. 2. Left: Absorption spectra of the modulation-doped sample 3 for different temperatures (Dashed: 10 K; Full: 60 K; Dotted: 120 K; Dash-dotted: 240 K). Right: the absorption of sample 4 whose population is optically tuned for different pump powers (2, 5, 15, and 50 mW) at $T=8$ K, corresponding to estimated carrier densities of 7×10^9 , 1.7×10^{10} , 5×10^{10} , and 1.7×10^{11} cm $^{-2}$, respectively.

tude higher than the Mott transition in the bulk GaAs. By increasing the doping level, the degeneracy of impurity and conduction bands is expected. The same experiments were performed on a sample doped 4×10^{11} cm $^{-2}$ (sample 2). As shown in Fig. 3, the absorption spectra of sample 2 show only one peak, as expected. As also expected, the low-temperature spectrum is broadened on Fig. 3 compared to the one on Fig. 1 (12 meV versus 9.5 meV) showing the impurity band broadening. Conduction measurement could not be performed on this sample because of the presence of contact layers. As a conclusion, the Mott transition occurs in our 6 nm Si-doped GaAs/AlGaAs QWs between donor concentrations of 2×10^{11} and 4×10^{11} cm $^{-2}$. This depends on the donor distribution in the well and thus on the growth condi-

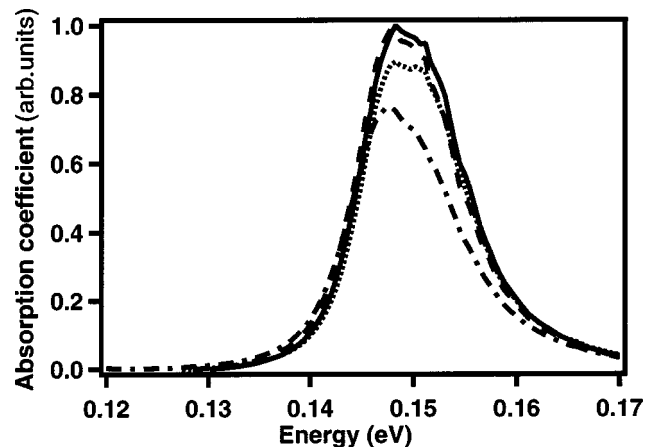


FIG. 3. Absorption spectra of 4×10^{11} cm $^{-2}$ δ -doped sample 2 for different temperatures (Dashed: 10 K; Full: 60 K; Dotted: 120 K; Dash-dotted: 240 K).

tions. Indeed, the relevant factor is the bulk concentration, which is in cm^{-3} . In our case, the Mott transition occurs between about 10^{18} and $2 \times 10^{18} \text{ cm}^{-3}$.

We used well known models to fit the spectra. Given the structure, a variational method was used to calculate the donor levels.¹⁵ The trial function of the ground impurity level $1s$ is based on the ground level of the well E_0 , and the one of the excited level $2p$ is based on the first excited level of the well E_1 , according to their respective symmetry. Given the energy levels, populations can be derived. The broadening of the impurity band is evaluated by a tight-binding model considering only the distance between two impurities. The contribution of each transition is given by a Lorentzian. The homogenous broadening and the temperature shift of the transitions are extracted as phenomenological parameters from the experiment performed on sample 3, in which the intersubband line shape is not affected by impurity-state absorption.

Information on the impurity distribution in the well can be deduced from the spectra. The spectrum at is the $1s \rightarrow 2p_z$ transmission spectrum because, as explained previously, the ground state E_0 is empty. It is thus only related to the impurity distribution.¹⁵ The variational calculations show that the binding energy depends on the position of the donors in the well, being low for impurities near the edges and maximum in the center. In Fig. 4, the 10 K spectrum of sample 5 is asymmetric. It can be explained by a particular distribution of the donors not only in the central third of the well, but also decreasing to zero toward the edge. This phenomenon is due to the Si segregation which is sensible to the growth conditions (such as the growth temperature). Indeed, a good agreement with the experimental results on sample 5 is obtained only for a QW doped in the central third and with a linear decrease of the doping in the edge third (inset of Fig. 4). The tail at high energy is due to transitions to the continuum above the well, which are not taken into account by the calculation. This absorption at 10 K can thus become an efficient, simple, and nondestructive way to measure the doping segregation in the wells. A classical method to know the composition of a multilayer is the secondary ion mass spectroscopy method. However, it is not precise enough to

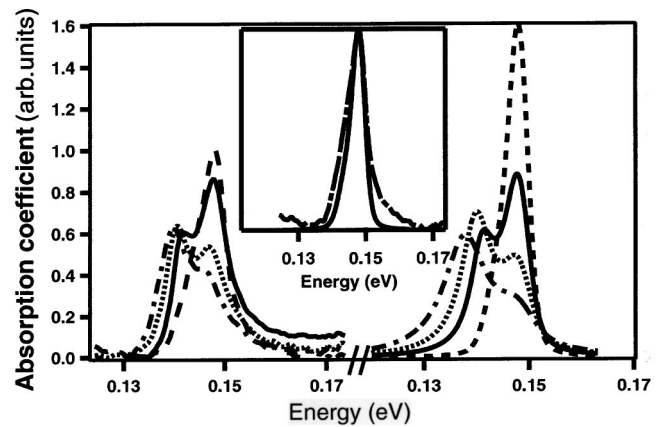


FIG. 4. Left: Spectra of sample 5 multi-QW structure for different temperatures (Dashed: 10 K; Full: 60 K; Dotted: 120 K; Dash-dotted: 240 K). Right: Model calculation of the absorption spectra of sample 5 for different temperatures (Dashed: 10 K; Full: 60 K; Dotted: 120 K; Dash-dotted: 240 K). Middle: (dashed curves of left and right figures). Experiment and theory at 10 K for comparison (Dash-dotted: experiment; Full: theory)

give us the distribution inside a QW of only 6 nm and it is a destructive method.

In conclusion, Mott transition was observed in a two-dimensional confined structure with the persistence of the impurity band at a doping level of $2 \times 10^{18} \text{ cm}^{-3}$, which is two orders of magnitude higher than in bulk GaAs. This effect, theoretically expected, had never, to our knowledge, been observed before.

The transition between impurity levels, only at low temperature, is directly related to the spatial distribution of the donors inside the QW. The observation of the absorption spectra is thus a simple, nondestructive, and accurate method to characterize the diffusion of donors in the wells and improve the molecular-beam epitaxy process. The understanding of Mott transition in QWs is also fundamental in the development of intersubband transition devices such as QWIPs.

¹D. Belitz and T. R. Kirkpatrick, *Rev. Mod. Phys.* **66**, 261 (1994).

²E. Moselkilde, *Physics Laboratory III: Linear and nonlinear acoustoelectric effects in heavily doped GaAs epitaxial single crystal*, Technical University of Denmark, Lyngby, 1977.

³G. E. Stillman, C. M. Wolfe, and J. O. Dimmock, *J. Phys. Chem. Solids* **31**, 1199 (1970).

⁴O. V. Emel'yanenko *et al.*, *Sov. Phys. Solid State* **7**, 1063 (1965).

⁵G. Bastard, *Phys. Rev. B* **24**, 4714 (1981).

⁶M. Hofmann, M. Bockstedte, and O. Pankratov, *Phys. Rev. B* **64**, 245321 (2001).

⁷J. Serre, A. Ghazali, and A. Gold, *Phys. Rev. B* **39**, 8499 (1989).

⁸M. Olszakier *et al.*, *Phys. Rev. Lett.* **62**, 2997 (1989).

⁹I. Galbraith, P. Dawson, and C. T. Foxon, *Phys. Rev. B* **45**, 13 499 (1992).

¹⁰M. Helm *et al.*, *Phys. Rev. B* **43**, 13 983 (1991).

¹¹M. Helm, W. Hilber, T. Fromhertz, F. M. Peeters, K. Alavi, and R. N. Pathak, *Phys. Rev. E* **48**, 1601 (1993).

¹²A. Harwit and J. S. Harris Jr., *Appl. Phys. Lett.* **50**, 685 (1987).

¹³M. M. Feyer, S. J. B. Yoo, R. L. Byer, A. Harwit, and J. S. Harris, *Phys. Rev. Lett.* **62**, 1041 (1989).

¹⁴M. Hauke, *J. Appl. Phys.* **84**, 2034 (1998).

¹⁵P. Jiang and W. C. Kok, *J. Appl. Phys.* **90**, 1271 (2001).